

# We are IntechOpen, the world's leading publisher of Open Access books Built by scientists, for scientists

5,500

Open access books available

136,000

International authors and editors

170M

Downloads

Our authors are among the

154

Countries delivered to

TOP 1%

most cited scientists

12.2%

Contributors from top 500 universities



WEB OF SCIENCE™

Selection of our books indexed in the Book Citation Index  
in Web of Science™ Core Collection (BKCI)

Interested in publishing with us?  
Contact [book.department@intechopen.com](mailto:book.department@intechopen.com)

Numbers displayed above are based on latest data collected.  
For more information visit [www.intechopen.com](http://www.intechopen.com)



# Medical Image Classification Using the Discriminant Power Analysis (DPA) of Discrete Cosine Transform (DCT) Coefficients

*Nasser Edinne Benhassine, Abdelnour Boukaache  
and Djalil Boudjehem*

## Abstract

Medical imaging systems are very important in medicine domain. They assist specialists to make the final decision about the patient's condition, and strongly help in early cancer detection. The classification of mammogram images represents a very important operation to identify whether the breast cancer is benign or malignant. In this chapter, we propose a new computer aided diagnostic (CAD) system, which is composed of three steps. In the first step, the input image is pre-processed to remove the noise and artifacts and also to separate the breast profile from the pectoral muscle. This operation is a difficult task that can affect the final decision. For this reason, a hybrid segmentation method using the seeded region growing (SRG) algorithm applied on a localized triangular region has been proposed. In the second step, we have proposed a features extraction method based on the discrete cosine transform (DCT), where the processed images of the breast profiles are transformed by the DCT where the part containing the highest energy value is selected. Then, in the feature's selection step, a new most discriminative power coefficients algorithm has been proposed to select the most significant features. In the final step of the proposed system, we have used the most known classifiers in the field of the image classification for evaluation. An effective classification has been made using the Support Vector Machines (SVM), Naive Bayes (NB), Artificial Neural Network (ANN) and  $k$ -Nearest Neighbors (KNN) classifiers. To evaluate the efficiency and to measure the performances of the proposed CAD system, we have selected the mini Mammographic Image Analysis Society (MIAS) database. The obtained results show the effectiveness of the proposed algorithm over others, which are recently proposed in the literature, whereas the new CAD reached an accuracy of 100%, in certain cases, with only a small set of selected features.

**Keywords:** medical images, breast cancer, pectoral muscle removal, discrete cosine transform, classification, SVM, KNN, ANN

## 1. Introduction

Cancer remains the killer disease in the world, and currently it has become a dangerous public health problem in many countries. In all kinds of cancer, the

problem arises when cancer cells begin to grow in uncontrolled manner or do not die when they should do so. In addition, breast cancer is a malignant tumor that is considered the most common type of cancer occurs in women and the second type of cancer in general. It has been announced, that more than 2 million new cases have been registered worldwide in 2018 [1]. Awareness of symptoms and the need for screening are very important to reduce the risk of cancer [2].

In medical imaging, it has been shown that early detection and proper treatment of breast cancer reduces the mortality rate by 20–40% [3]. The use of Mammography, represents an effective tool in the early detection of the breast cancer. As a result, many computer-aided diagnostic (CAD) systems have been developed using digital image processing techniques applied to mammography images. These systems are very useful to help radiologists in the early detection of breast cancers and then to classify the breast tumor as malignant or benign [4–6].

In general, any CAD system can be composed of three different steps: image pre-processing step, features extraction and selection step and finally the classification step. For the breast cancer detection and classification, many works have been presented to improve the efficiency of the CAD systems. In the pre-processing step, the pectoral muscle removal and the region of interest (ROI) extraction rest a big challenge. Numerous segmentation algorithms have been also proposed to suppress the pectoral muscle [7–10]. However, there is no universal segmentation algorithm that can give acceptable results for all cases.

In the features extraction step, different techniques can be used like, shape and texture features [11, 12], morphological and texture features [13], independent component analysis (ICA) [14], the discrete cosine transform (DCT) [15], the discrete wavelet transform (DWT) [16, 17] and other transforms. In [18], the authors used non-subsampled contourlet transformation together with discrete wavelet transform with gray level co-occurrence matrix for texture features extraction. Salabat Khan et al. used a Gabor filter bank (GBF) optimized by Particle Swarm Optimization (PSO) for the extraction of Gabor characteristics [19]. Mughal B et al. used the backpropagation neural network on the hat transformation with gray level co-occurrence matrix (GLCM) features [20].

For the classification step, the most used classifiers are Artificial Neural Networks (ANN), Support Vector Machine (SVM), Naïve Bayes (NB) and  $k$ -Nearest Neighbors (KNN). Recently, in [21], the authors used deep learning architecture that is known as You Only Look Once (YOLO). In [22], the authors proposed a deep Convolutional Neural Network (CNN). In [23], Agnes et al., used Multiscale All Convolutional Neural Network (MA-CNN).

In this chapter, we propose a new computer-aided diagnostic system to classify breast tumors as malignant or benign. In the pre-processing step, we have proposed a new algorithm to select a limited triangular region that contains the pectoral muscle to be eliminated, and then apply the SRG segmentation algorithm. Features extraction and selection are also very important processes to improve the system performances in classification and pattern recognition methods. By using discrete Fourier transform or discrete cosine transform, we obtain a frequency domain representation of the image that can be considered as a set of features for pattern recognition problems. While the FFT give complex coefficients, the DCT provide real values in the frequency domain. We have used the DCT transform for feature extraction, and we have proposed the selection of the most significant features using the (DPA) algorithm [24]. Finally, we have evaluated the performances of the algorithm using SVM, ANN, NB and KNN classifiers and the MIAS database mammograms [25].

## 2. The proposed CAD system

The proposed Computer-aided diagnostic system (CAD) that is used to classify the breast tissue in mammograms as malignant or benign is divided into three basic processing steps as shown in **Figure 1**.

### 2.1 Image pre-processing

This step represents an important one in most CAD systems. The image pre-processing helps strongly in the selection of the region of interest (ROI) that contains the abnormalities. It is performed to remove the unwanted objects, which include artifacts, labels, background noises and to suppress the pectoral muscle (**Figure 2**). The use of efficient image processing methods is an indispensable step for achieving a high accuracy classification in CAD systems for the diagnosis of breast cancer.

#### 2.1.1 Noise removal

There are various types of noises affected on mammogram images, such as Salt and pepper noise, Speckle noise, Gaussian noise and Poisson noise. Therefore, it is important to remove the noises to enhance the image quality on the preprocessing step. Traditionally, the median filter is a well-known used filter for this kind of noises, due to its nonlinear behavior, its simplicity and capability to preserve edges [26]. The median filter replaces each pixel value by the median of all the neighboring pixels values in a window. In this chapter, we used a (3x3) median filter to reduce noise in the mammogram images.

#### 2.1.2 Artifacts suppression and background separation

In order to remove all unwanted objects in the selected image and separate the breast profile, we follow the next four steps:

Step (1) Thresholding of the mammogram image by 0.0706 normalized value.

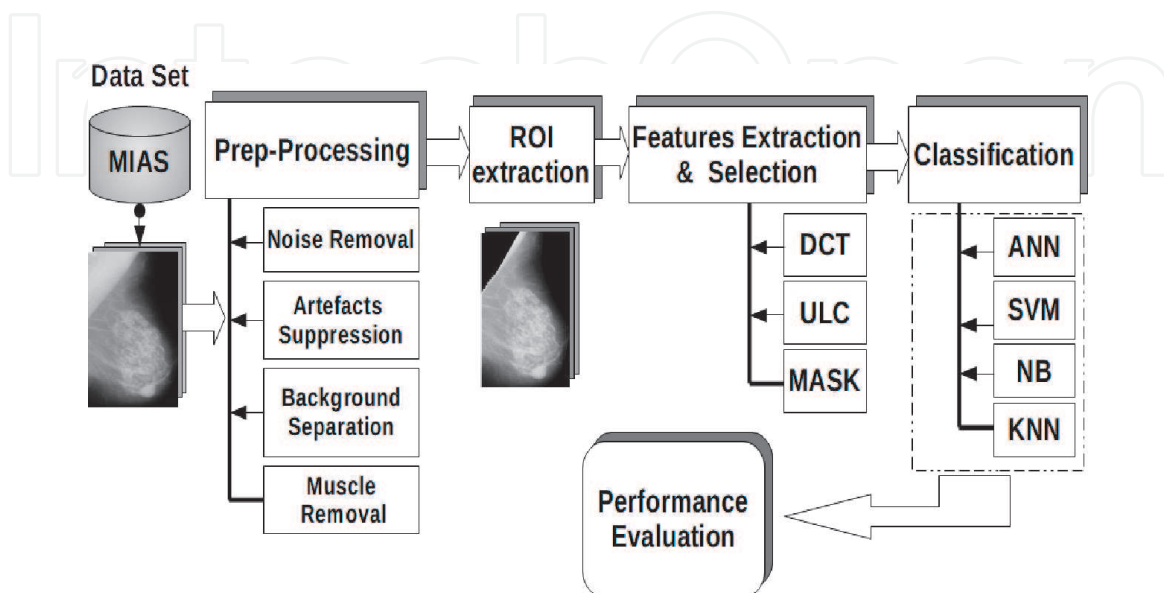


**Figure 1.**  
Flow chart of CAD system for breast cancer classification.

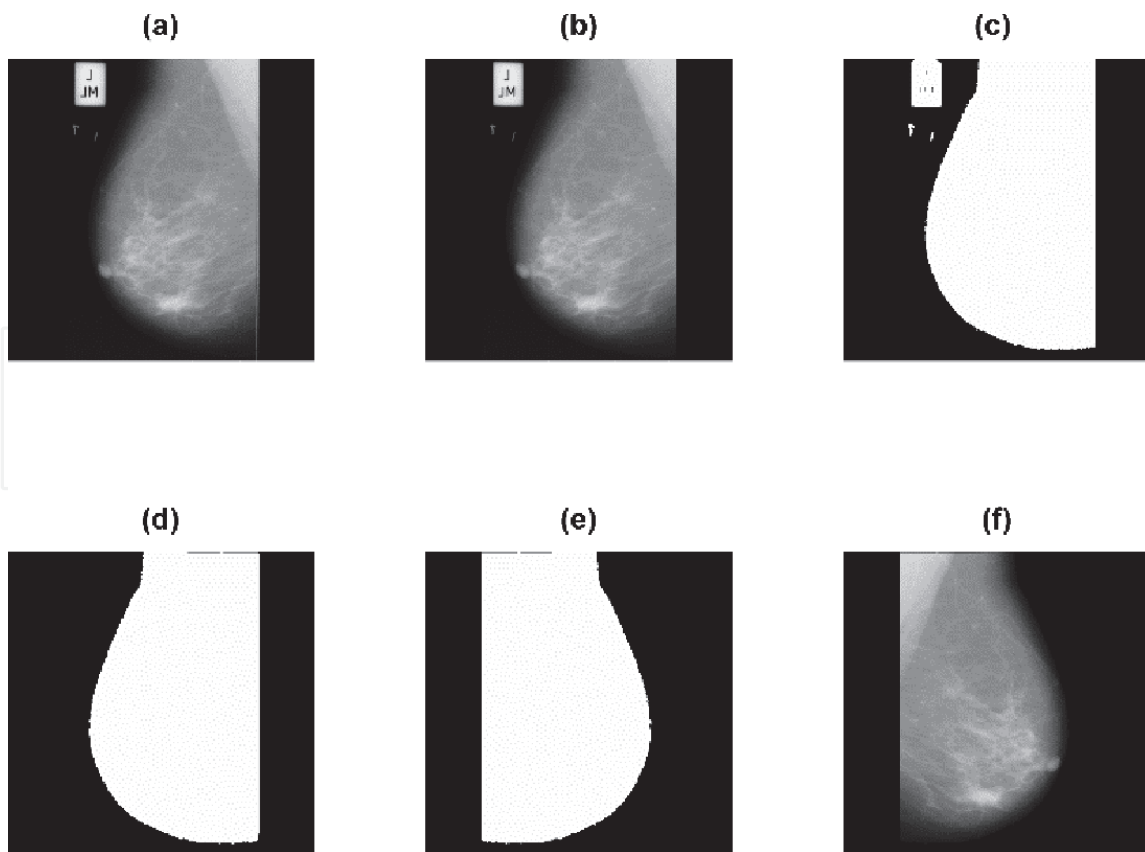


**Figure 2.**  
The preprocessing steps of mammogram image: (a) original image, (b) noise removed image, (c) binary image, (d) largest area, (e) image right flipped, (f) parenchyma of the breast.

- Step (2) Mark all regions in the thresholded image (i.e., Artifacts, labels, ...).
- Step (3) Calculate the area of each region, and select the largest one.
- Step (4) The result of the step (3) is then used as a mask of the original grayscale mammography image.

### 2.1.3 Localization and extraction of the pectoral muscle

In the mammogram preprocessing, the identification and extraction of the pectoral muscle is one of the major challenges in Medio lateral Oblique (MLO) view. It could be noticed here, that this step is important to improve the diagnostic accuracy of the CAD system. The difficulty in removing the pectoral muscle is due to the following reasons [27]:

- Homogeneous area situated in the top left/right corner contains the brightest pixels in the image.
- The pectoral muscle boundary shape is concave, convex or a mixture of both of them.
- The density of the pectoral muscle area appears at approximately with similar density as the dense tissues.
- Varying position, size, shape and texture from image to image.



In this chapter, we present a new algorithm for pectoral muscle suppression, this operation is based on the Localization of the triangular region that contains the Pectoral Muscle, where the Seeded Region Growing (SRG) algorithm is invoked in this operation.

---

**Algorithm 1** Removal of the of pectoral muscle [15]

---

**Input:** MLO mammograms size of 1024x1024

- Step (1) All the right MLO mammograms are left-right flipped
  - Step (2) Divided MLO into four equal quadrants of 512x512 pixels.
  - Step (3) The upper left quadrant is cropped with removing the left background
  - Step (4) The result is divided diagonally into two equal triangles.
  - Step (5) Select the Seed point
  - Step (6) Apply the SRG in the upper left triangle ABC (that contains the Pectoral Muscle)
  - Step (7) Re-Construct the Image and removing all backgrounds
- 

**Output:** The region of interest (ROI)

---

Seeded Region Growing (SRG) is a useful image segmentation technique for medical images that is initially proposed by R. Adams *et al.* [28]. This technique is robust, fast and consists of three major steps: seed selection, region growing, and region merging.

The advantage of applying the (SRG) method into the localized triangular ABC region (**Figure 3**) is to remove only the pectoral muscle, without completely suppressing the triangular region as in some other methods. **Figures 3–5** show a visual scheme of the proposed algorithm.

The Seed point is selected automatically by considering the results obtained from step (4) of algorithm 1.

**Figure 5(a)** shows the cropped image, where **Figure 5(b)** shows the selected region of interest (ROI). All obtained (ROI) images are resized in order to get the same dimension.

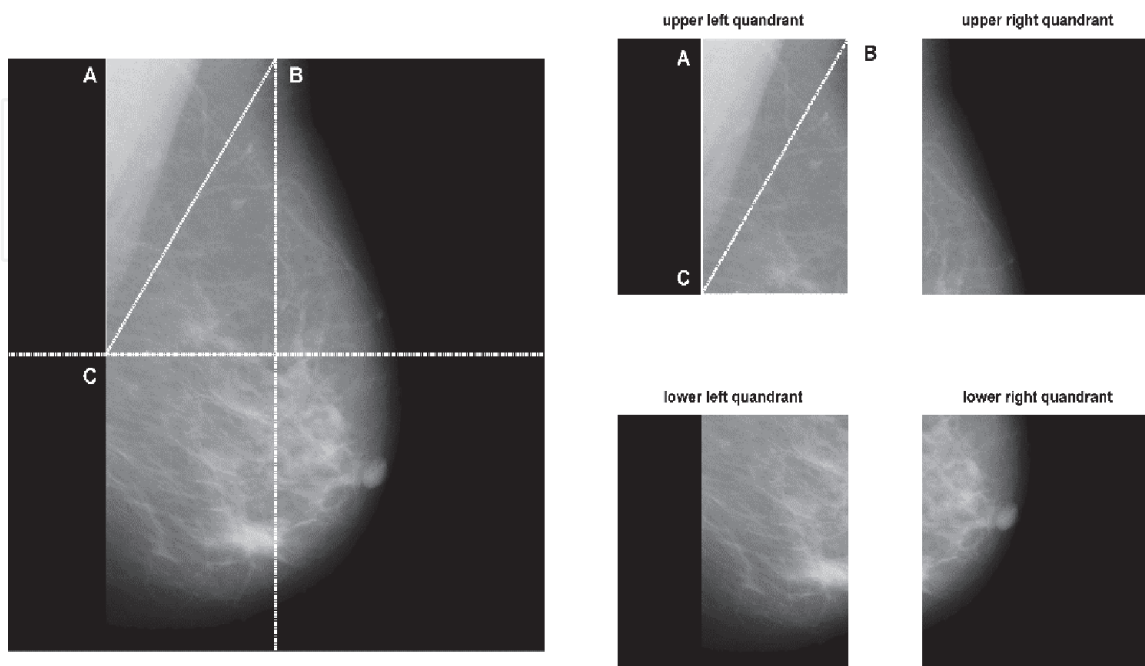


**Figure 3.** Localization of the ABC triangle in the left upper quadrant.

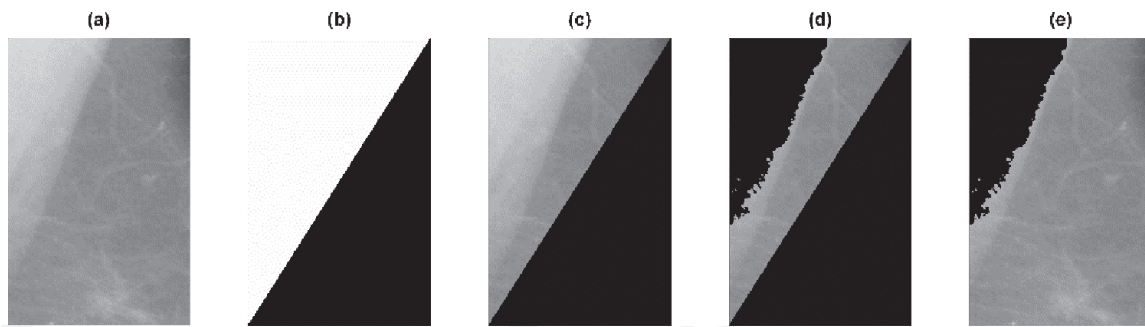


**Figure 4.** Pectoral muscle segmentation steps: (a) mammogram top left quadrant, (b) triangular mask, (c) masked top left quadrant, (d) suppression of the pectoral muscle, (e) cropped top left quadrant without pectoral muscle.

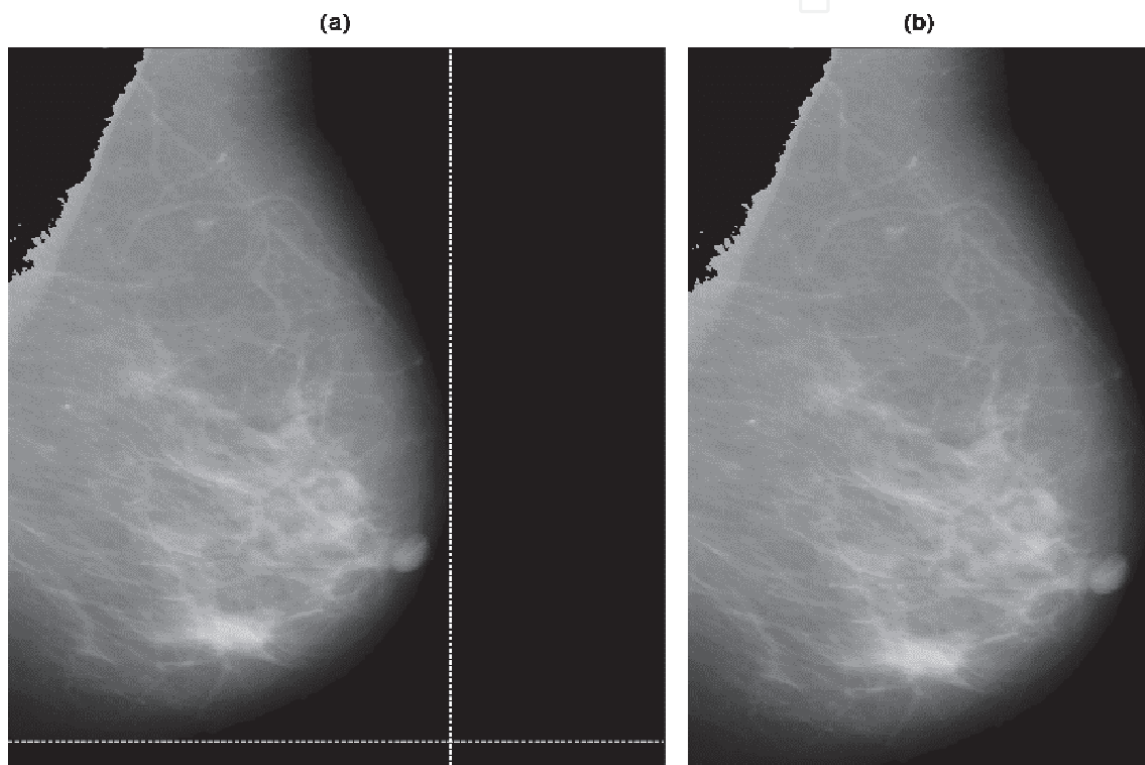


**Figure 5.** Identification of the region of interest (ROI). (a) Cropped image, and (b) Selected region of Interest (ROI).

## 2.2 Frequency domain features extraction and selection

Features extraction plays an essential role, and a challenging step in the accurate classification and diagnostic rate of mammograms. In this chapter, we have used features extracted from the image in the frequency domain representation. The most used transform to this domain is the discrete Fourier transform with its fast algorithm (FFT) [29]. In classification problems, for example, Fourier descriptors have been used for pattern recognition [30, 31]. Another interesting transform is the discrete cosine transform (DCT) which decomposes the image on a set of cosine functions. It provides a real representation of the image contrary to the FFT, which give complex coefficients.

The frequency domain features are very used in the classification and pattern recognition field. However, the hard task is the selection of the transformed

coefficients, while these coefficients do not have the same aptitude to discriminate between the different classes. However, the use of the standard approaches to select these coefficients are not always efficient in selecting the most discriminative coefficients. In this chapter, we present a novel features extraction technique that is composed of two phases. In the first one, the discrete cosine transforms (DCT) is applied on all the obtained regions of interest (ROI), and then the low frequency coefficients in the upper left corner (ULC) are retained. In the second phase, a combination of the retained frequency coefficients with the discriminative power coefficients algorithm [24] is proposed to calculate the discrimination power matrix, which is given by the ratio between the two variances, the between-class variance and the within-class variance. Where, high classification accuracies are represented by high rate values.

### 2.2.1 Discrete cosine transform (DCT)

This mathematical tool transforms any signal or image from the spatial domain to frequency domain. It has been widely used in digital signal and image processing, where its major advantages over the FFT reside in giving real coefficients. In addition, it concentrates the information in the low frequency region. Fast implementation can be obtained by using the FFT algorithm [29] which make the use of this transform very simple in real-time applications. It is defined by Eq. (1):

$$F(u, v) = \frac{1}{\sqrt{MN}} \alpha(u)\alpha(v) \sum_{i=0}^{M-1} \sum_{j=0}^{N-1} I(i, j) \cos\left(\frac{(2i+1)u\pi}{2M}\right) \cos\left(\frac{(2j+1)v\pi}{2N}\right) \quad (1)$$

with  $0 \leq u \leq M$ ,  $0 \leq v \leq N$ , and  $\alpha(u)$ ,  $\alpha(v)$  are defined by Eq. (2), Eq. (3)

$$\alpha(u) = \begin{cases} \frac{1}{\sqrt{2}} & u = 0 \\ 1 & \text{otherwise} \end{cases} \quad (2)$$

$$\alpha(v) = \begin{cases} \frac{1}{\sqrt{2}} & v = 0 \\ 1 & \text{otherwise} \end{cases} \quad (3)$$

and  $F(u, v)$  is the DCT coefficient matrix of the image  $I(i, j)$ .

After the calculation of the DCT coefficients, we retain only the 512x512 region in the upper left corner (ULC coefficients). In the feature's selection step, a new most discriminative power analysis (DPA) algorithm has been proposed to select the most significant features that have the high discrimination power (DP) values.

### 2.2.2 Discriminative power analysis of DCT coefficients

The calculation of the (DP) for each transformed coefficient is shown in the (DCT-DPA) algorithm shown below. Considering an image  $I_{ij}$  of size  $N \times M$ .  $F_{uv}$  are the transformed coefficient by the 2D-DCT. The used database has  $C$  classes each is composed of  $S$  training images. Consequently, a total of  $C \times S$  training images are used.



---

**Input:** The number of used classes  $C$ , the training images' number  $S$  of each class  
The matrix  $Im=zeros(N, M)$

---

**Require:** Pre-processing function  $PPf()$  and the bi-dimensional DCT ( $DCT2$ ).

---

```

(1)   For      every class  $c \ \forall c \leq C$ 
(2)   |        $S_{ij} = Im;$ 
(3)   |       For  every image  $s (I_{ij}(S, C)) \ \forall s \leq S$ 
(4)   |       |    $I_{ij}(S, C) \leftarrow PPf(I_{ij}(S, C))$  // call  $PPf()$ 
(5)   |       |    $F_{uw}(S, C) \leftarrow DCT2(I_{ij}(S, C))$ 
(6)   |       |    $S_{ij} \leftarrow S_{ij} + F_{uw}(S, C)$  //sum of images of each class
(7)   |       End
(8)   |        $M_{ij}^c \leftarrow S_{ij}/S$  // the mean value of each class
(9)   |        $V_{ij}^c = Im;$ 
(10)  |       For  every image  $s (I_{ij}(S, C)) \ \forall s \leq S$ 
(11)  |       |    $I_{ij}(S, C) \leftarrow PPf(I_{ij}(S, C))$ 
(12)  |       |    $F_{uw}(S, C) \leftarrow DCT2(I_{ij}(S, C))$ 
(13)  |       |    $V_{ij}^c \leftarrow V_{ij}^c + (F_{uw}(S, C) - M_{ij}^c)^2$  // the variance of each
(14)  |       |   class
(15)  |       End
(16)  |        $M_{ij} \leftarrow \frac{1}{C} \sum_{c=1}^C M_{ij}^c$  // the mean of all training samples
(17)  |        $V_{ij}^w \leftarrow \frac{1}{C} \sum_{c=1}^C V_{ij}^c$  // average the variance of all the classes
(18)  |        $V_{ij}^B = Im$ 
(19)  |       For  every class  $c \ \forall c \leq C$ 
(20)  |       |   For  every image  $s (I_{ij}(S, C)) \ \forall s \leq S$ 
(21)  |       |   |    $I_{ij}(S, C) \leftarrow PPf(I_{ij}(S, C))$ 
(22)  |       |   |    $F_{uw}(S, C) \leftarrow DCT2(I_{ij}(S, C))$ 
(23)  |       |   |    $V_{ij}^B \leftarrow V_{ij}^B + (F_{uw}(S, C) - M_{ij})^2$  // the
(24)  |       |   |   variance of the database samples
(25)  |       |   End
(26)  |       End
(26)  |        $Dp(i, j) = V_{ij}^B / V_{ij}^w$  //  $1 \leq i \leq M, 1 \leq j \leq N$ 
output   $Dp(i, j)$  // the discrimination power matrix
    
```

---

The  $Dp(i, j)$  matrix is defined as the ratio of between-class variance and within-class variance. Large values of DP imply a large discrimination power of the coefficients. The selection of the DCT coefficients is made in an adaptive way according to their corresponding DP values, where the DCT coefficients with higher DP are preserved [24]. The  $Dp(i, j)$  matrix is then transformed into a column vector that will be sorted in descending order. Therefore, the number  $k$  selected among the highest values, defines the number of the features to be used by the classifier. By setting the positions of selected features as ones and the others as zeros, we create a mask that can be used later in the selection process of the classification step. Alternatively, we can use a thresholding step of the  $DP$  matrix to create a mask that contain  $k$  elements as follows:

$$Mask(i, j) = \begin{cases} 1 & Dp(i, j) \geq T \\ 0 & otherwise. \end{cases} \quad (4)$$

with  $1 \leq k \leq M \times N$  and  $T$  is the  $k^{th}$  highest value in the  $DP$  matrix.

## 2.3 Classification

The classification is the last step to identify if the breast tumor is benign or malignant. It plays a vital role in the medical image diagnosis field. Therefore, the images need to be classified with maximum accuracy. As a result, some automated classification methods have been proposed. In this part, we presented some of these classifiers including NB, SVM, ANN, and KNN that are used for breast cancer detection. A brief description of these algorithms will be presented as well as their advantages and disadvantages.

### 2.3.1 The support vector machine (SVM)

SVMs are a set of machine learning algorithms that help solve problems associated with classification, regression, and fault detection. They are considered to be among the algorithms that are distinguished by their strong theoretical guarantee and their great flexibility. They are also considered among the easiest algorithms in terms of ease of use even in cases where there is a little knowledge of data extraction.

The SVMs use increases widely in medical imaging field especially for breast cancer diagnosis [32]. The basic principle of SVM in this chapter is to separate and classify images into two categories malignant and benign using a hyperplane decision boundary, ensuring a maximum distance between different data sets and the boundary separating them. For linearly separable data, the hyperplane decision boundary is given by [33]:

$$g(x) = w^t x + b = \sum_{i=1}^n w_i^t x_i + b \quad (5)$$

where  $x$  is the input data set vector  $w$  is ( $n$ ) dimensional and  $b$  is a bias. The main advantages of the (SVM) classifier can generally be listed as follows [15]:

1. SVM generally gives good accuracy with less memory use.
2. It works very well in cases where the separation margin between data sets is clear.
3. It can also solve any complex problem by specifying different kernel function.

The main disadvantages of the SVM algorithm are the difficulty of choosing the appropriate kernel function and the long training time for large datasets.

### 2.3.2 Artificial neural network (ANN)

The artificial neural networks are feed-forward networks that can be trained to classify inputs according to target classes. Generally, a neural network is composed of three layers: an input layer, a hidden layer and an output layer [34]. Usually, only the input and output signals of the network are already known [17]. The process of training an artificial neural network before setting it up represents a serious operation and affects directly the final obtained results. This operation depends on some constraints like the initial parameters setting, the use weights, bias and finally the used algorithm learning rate. To adjust the weights of the ANN, one can use some

learning methods like the back-propagation or an optimization algorithm. In this work, the input layer is based on the number of the features selected, the hidden layer contains 10 neurons, and finally the out layer.

### 2.3.3 Naive Bayes classifier (NB)

Naive Bayes is becoming increasingly popular in many areas, it has shown excellent performances for classification tasks. It is a simple probabilistic classifier based on Bayes' theorem, which is based on conditional probabilities [35]. A Naive Bayes classifier assigns a new observation to the most probable class, assuming the features are conditionally independent for a given the class value. It is easy and fast to predict the class of the test data set, but their biggest disadvantage is its requirement to an independent predictor [15].

### 2.3.4 K-nearest neighbors (KNN)

K-nearest neighbors' classifier is a statistical non-parametric method that is used for both classification and regression [36]. In its simplest version, the KNN takes an arbitrary number ( $k$ ) of neighbors nearer from the training set, and for each test point we start by determining all of its  $k$ -nearest neighbors among the learning points. The class that we assign to the new point is then the more frequent. In the KNN the Euclidean distance metric is used and it is given by:

$$d(x, y) = \sqrt{\sum_{i=1}^k (x_i - y_i)^2} \quad (6)$$

where  $x_i$  is the test sample with  $k$  features and  $y_i$  specified the training samples with  $k$  features. The Advantages of using KNN are that it is robust to noisy training data, and it is effective when used with large training data. On the other hand, it needs to determine the number of nearest neighbors ( $k$ ) and the distance-based learning.

## 3. Results and discussions

To validate the proposed system, experiments were performed on the digital mammography images from the Mammographic Image Analysis Society (MIAS) database [25]. The MIAS database is a standard and publicly available database of digital mammogram images. Each mammogram is  $1024 \times 1024$  pixels of size with a resolution of 200 microns. MIAS contains 322 mammograms for right and left breast of 161 patients in the mediolateral oblique (MLO) view, 61 mammograms were diagnosed as benign, 54 as malignant and 207 normal. The performance of the proposed method has been tested based on algorithms' accuracy, sensitivity and specificity using the following expressions:

$$\text{Sensitivity} = \frac{TP}{TP + FN} \times 100 (\%) \quad (7)$$

$$\text{Specificity} = \frac{TN}{TN + FP} \times 100 (\%) \quad (8)$$

$$\text{Accuracy} = \frac{TN + TP}{TN + FN + FP + TP} \times 100 (\%) \quad (9)$$

Where:

*TN* (True Negative) is the number of a benign classified as benign.

*TP* (True Positive) is the number of a malignant classified as malignant.

*FN* (False Negative) is the number of a benign classified as malignant.

*FP* (False Positive) is the number of a malignant classified as benign.

In this test, we have calculated the *D<sub>p</sub>* matrix using a set of 50 images of benign mammograms and another 50 images of malignant mammograms. These images are randomly selected as shown in the DCT-DPA algorithm. It is very important to select an equal number of samples from each class. The increase of the number of samples implies an increase of the efficiency of the performance of the classifier. However, the best results in this test are obtained using 50–50 mammogram images. Then, the database is randomly divided into train and test data sets. We have taken 113 (ROIs) divided into 70% for training and 30% for testing. The given results are the average of ten runs.

**Table 1** shows a comparison of the measured performances of the SVM, ANN, NB and KNN classifiers. It is observed that the classification accuracy can reach 100% for the (ANN) classifier, is 98.8, 96.7%, 87.3% for SVM, NB and KNN

Classifiers	Sensitivity (%)	Specificity (%)	Accuracy (%)
KNN	91.05	82.67	87.3
NB	97.9	97.3	96.7
SVM	99.5	98.1	98.8
ANN	<b>100</b>	<b>100</b>	<b>100</b>

Abbreviations: ANN, artificial neural network; SVM, support vector machines; NB, Naive Bayes, KNN, K-nearest neighbors.

**Table 1.**  
 Classification performance using ANN, SVM, NB and KNN classifiers.

ULC size	N. of Features	ANN	SVM	NB	KNN
		Accuracy (%)			
128x128	60	95.6	86.76	90.6	77.9
	80	96.5	90.3	92.3	78.5
	100	98.2	94.7	92.6	79.7
256x256	60	98.2	91.2	93.2	75.0
	80	97.3	91.7	95.3	75.8
	100	98.2	93.8	93.8	76.1
512x512	60	98.2	92.1	93.8	77.0
	80	99.1	97.3	97.3	79.1
	100	<b>100</b>	<b>98.8</b>	<b>97.6</b>	<b>87.3</b>
1024x1024	60	98.2	92.6	93.1	82.6
	80	96.5	88.5	93.2	83.5
	100	97.3	91.7	94.1	85.6

Abbreviations: ANN, artificial neural network; SVM, support vector machines; NB, Naive Bayes, KNN, K-nearest neighbors.

**Table 2.**  
 Classification accuracy with various sizes of ULC and different numbers of features. Where the best results are represented by bold values.

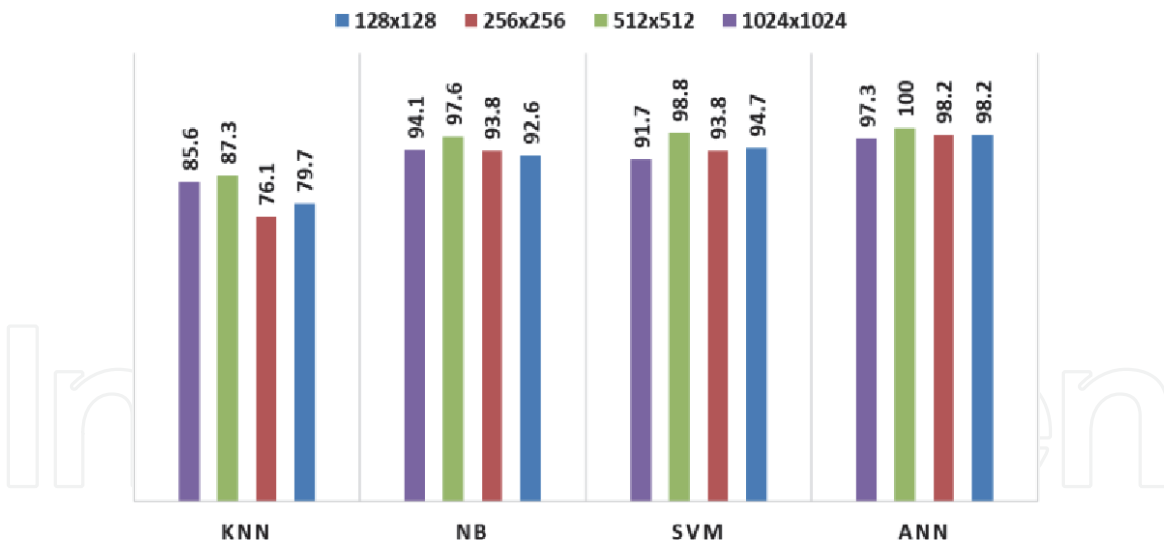


**Figure 6.**  
Classification accuracy performances vs. the ULC sizes with 100 features.

respectively. We have evaluated the classification performances of the proposed algorithm according to the number of the used features in the classification.

The SVM, ANN, NB and KNN classifiers are used to classify input images into benign or malignant. The sensitivity, accuracy and specificity are shown in **Table 2**. According to the results in **Table 2**, we can see that small number of features (100 features in this case) can achieve best performances in the case of 512x512 ULC size. In addition, we have studied the effect of the ULC size on the obtained results. The accuracy curve of the classification accuracy versus the ULC size is shown in **Figure 6**. The number of used features is 100 features.

**Figure 7** represents the variation of the classification accuracy according to different features' number with a fixed ULC size of 512x512. **Figure 8** demonstrates the classification performance of ANN using the confusion matrix for training, test and validation data.

To show the efficiency of the presented technique, **Table 3** shows a comparison between the results of the proposed algorithm with previous results, which are reported in the literature. We can see that the proposed CAD system gives better accuracy results compared to those obtained using the other methods.

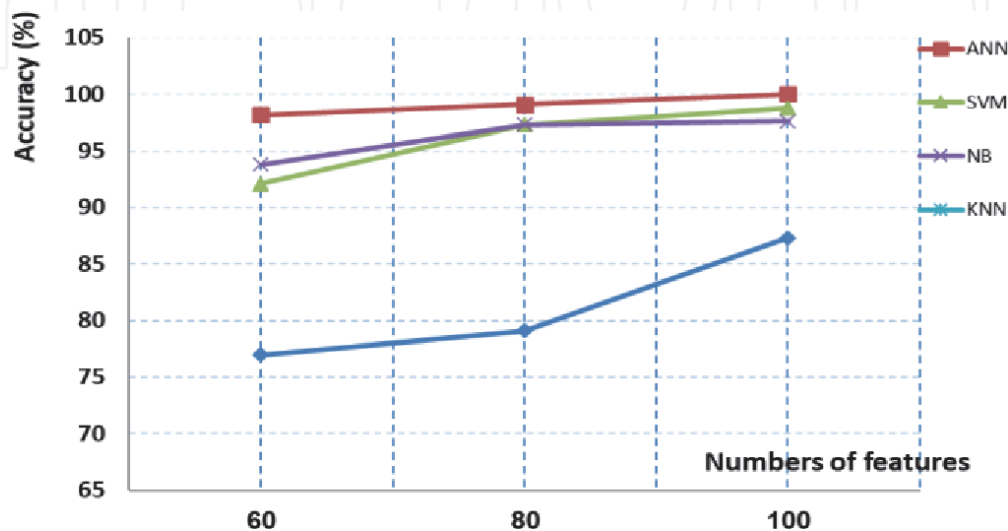


**Figure 7.**  
Classification performances vs. the number of features. (ULC size of 512x512).



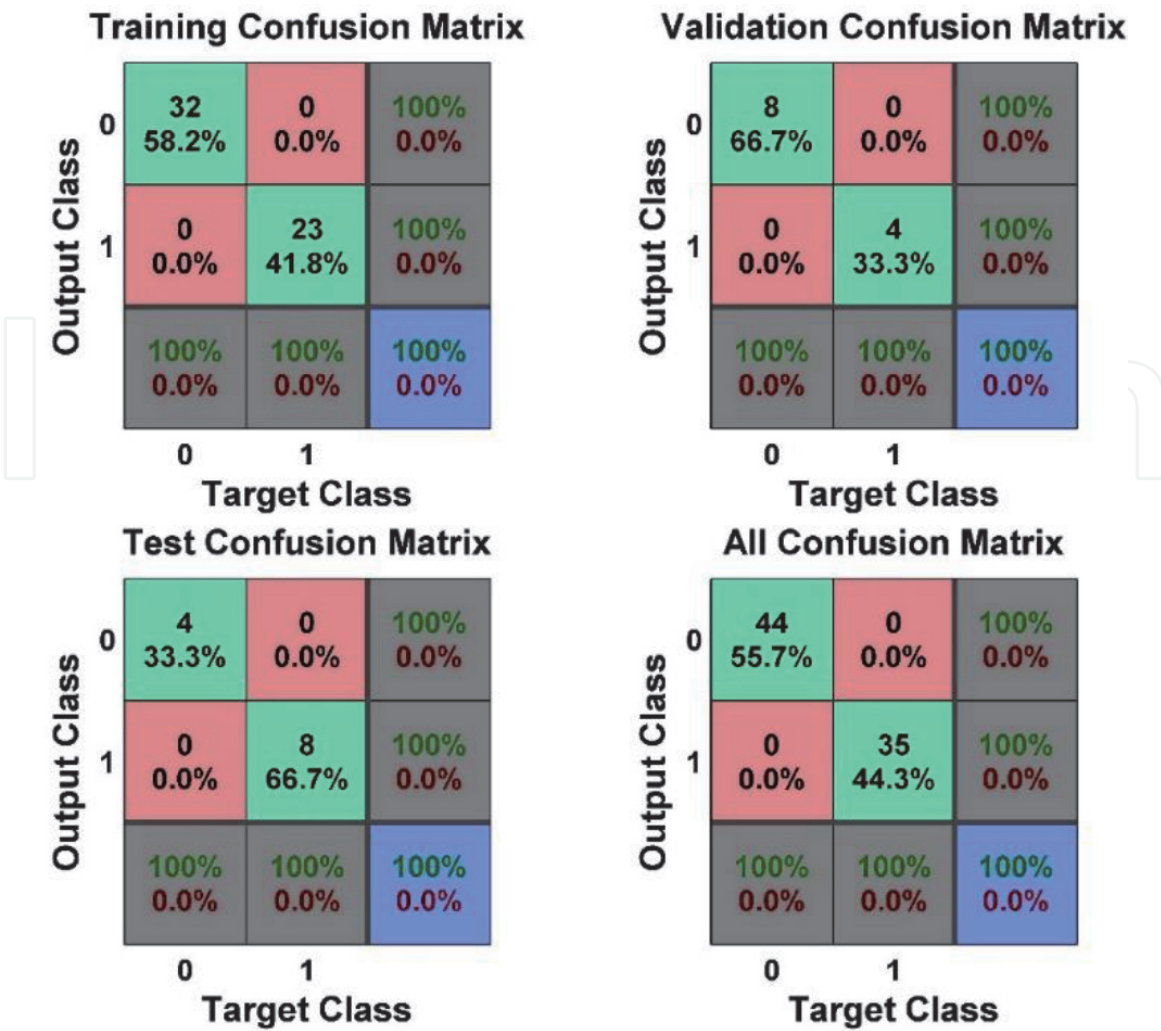


**Figure 8.**  
 Confusion matrix for training, test and validation data.

Authors	Year	Database	Classifier	Classes	Accuracy (%)
Lima [12]	2016	MIAS	SVM	2	94.1
Singh [37]	2017	MIAS	RF	2	97.3
Elmoufidi [38]	2017	MIAS	SVM	2	94.4
Mughal [20]	2018	MIAS	NNB	2	98.5
				2	95
Benzebouchi [22]	2019	MIAS	SVM	2	94.0
Benhassine [15]	2019	MIAS	ANN	2	100
			SVM		94.1
			NB		92.6
El-Sokary [39]	2019	MIAS	SVM	2	92.5
				3	90.0
Benhassine [17]	2020	MIAS	ANN	2	99.1
			SVM		99.4
			RF		98.2
			NB		97.7
Taifi [18]	2020	MIAS	SVM	2	94.1
			KNN	2	88.8

Authors	Year	Database	Classifier	Classes	Accuracy (%)
Luqman [40]	2020	MIAS	Deep Lab	2	95.0
		CBIS-DDSM	Mask-RCNN		98.0
Proposed method	2020	MIAS	ANN	2	100
			SVM		98.8
			NB		97.6
			KNN		87.3

Abbreviations: ANN, artificial neural network; SVM, support vector machines; NB, Naive Bayes; RF, random Forest; KNN,  $k$ -nearest neighbors; M-RCNN and Dee Lab (two deep learning-based instance segmentation Frameworks); Subset of CBIS-DDSM Curated Breast Imaging of DDSM (Digital Database for Screening Mammography).

**Table 3.**  
Comparison results of the proposed method with existing methods.

## 4. Conclusions

We have developed in the present chapter a new CAD system used for mammogram images classification. It consists of three main parts. First, we remove all unnecessary regions or objects from the input image, where we have proposed a mixed approach for pectoral muscle removing which can improve the diagnostic accuracy of the developed CAD system. Then, we have focused in our work on frequency domain features where we have used the discrete cosine transform (DCT). The extracted features are subject to a selection process that choose only the most important features. This step is done using the discriminant power analysis (DPA) algorithm. Finally, some of the most known classifiers in the field are used to make the final decision. The proposed system is evaluated on mammogram images from the MIAS database, where we have shown that a small number of selected features can give good results of the accuracy, sensitivity and specificity. The obtained results prove that the frequency domain features can give high performances especially with the use of the discrimination power analysis, and highlight the importance of DCT transform in recent artificial intelligence applications. The comparison of the obtained results with those obtained using recently proposed techniques shows the superiority of the proposed algorithm against the other methods.

### Author details


Nasser Edinne Benhassine<sup>1,2</sup>, Abdelnour Boukaache<sup>1</sup> and Djalil Boudjehem<sup>1\*</sup>

1 Advanced Control Laboratory (LABCAV), University of 8<sup>th</sup> May 1945, Guelma, Algeria

2 University center of Aflou, Algeria

\*Address all correspondence to: boudjehem.djalil@gmail.com

### IntechOpen

© 2020 The Author(s). Licensee IntechOpen. This chapter is distributed under the terms of the Creative Commons Attribution License (<http://creativecommons.org/licenses/by/3.0>), which permits unrestricted use, distribution, and reproduction in any medium, provided the original work is properly cited. 

## References

- [1] The World Health Organization (WHO): <http://www.who.int/mediacentre/factsheets/fs297/en/> [Accessed: 2018-10-28]
- [2] American Cancer Society, Breast Cancer Facts & Figures 2017–2018, Atlanta: *American Cancer Society, Inc.* 2017.
- [3] Jalalian A, Mashohor S, Mahmud R, Karasfi B, Saripan MI, Ramli AR. Computer-assisted diagnosis system for breast cancer in computed tomography laser mammography (CTLM). *J Digit Imaging*. 2017; 30:796–811
- [4] Pisano ED, Shtern F. Image processing and computer aided diagnosis in digital mammography: a clinical perspective. *Int J Pattern Recognit Artif Intell*. 1993; 7(06):1493–1503.
- [5] Giger ML, Karssemeijer N, Armato SG. Computer-aided diagnosis in medical imaging. *IEEE Trans Med Imaging*. 2001;20(12):1205–1208.
- [6] Vyborny CJ, Giger ML, Nishikawa RM. Computer-aided detection and diagnosis of breast cancer. *Radiol Clin North Am*. 2000;38(4):725–740.
- [7] Singh VP, Srivastava R. Content-based mammogram retrieval using wavelet based complete LBP and K-means clustering for the diagnosis of breast cancer. *Int J Hybrid Intell Syst*. 2017; 14:31–39.
- [8] Karssemeijer N. Automated classification of parenchymal patterns in mammograms. *Phys Med Biol*. 1998;43(2):365–378.
- [9] Xu W, Xia S, Duan H. A novel computer-aided diagnosis system of the mammograms. In: Huang DS, Li K, Irwin KGW, eds. *Intelligent Computing in Signal Processing and Pattern Recognition*. 2006;639–644.
- [10] Nagi J, Kareem SA, Nagi F, Ahmed SK. Automated breast profile segmentation for ROI detection using digital mammograms. *Biomedical Engineering and Sciences (IECBES)*; November 30–December 2, 2010; Kuala Lumpur, Malaysia: IEEE; 2010. p. 87–92
- [11] Zakeri FS, Behnam H, Ahmadinejad N. Classification of benign and malignant breast masses based on shape and texture features in sonography images. *J Med Syst*. 2012;36(3):1621–1627.
- [12] de Lima SM, da Silva-Filho AG, dos Santos WP. Detection and classification of masses in mammographic images in a multi-kernel approach. *Comput Methods Programs Biomed*. 2016; 134: 11–29.
- [13] Oliver A, Freixenet J, Marti R, et al. A novel breast tissue density classification methodology. *IEEE Trans Inf Technol Biomed*. 2008;12(1):55–65.
- [14] Campos LFA, Silva AC, Barros AK. Diagnosis of breast cancer in digital mammograms using independent component analysis and neural networks, vol 3773. *Iberoamerican Congress on Pattern Recognition*; November 15–18, 2005; Havana, Cuba; 2005:460–469.
- [15] Benhassine, N.E., Boukaache, A. and Boudjehem D. Classification of mammogram images using the energy probability in frequency domain and most discriminative power coefficients. *Int J Imaging Syst Technol*. 30:45–56, 2019. <https://doi.org/10.1002/ima.22352>.
- [16] Lahmiri S, Boukadoum M. Hybrid discrete wavelet transform and Gabor

filter banks processing for features extraction from biomedical images. *J Med Eng.* 2013; 2013:1–13.

[17] Benhassine, N.E., Boukaache, A. and Boudjehem D. A new CAD System for Breast Cancer Classification using Discrimination Power Analysis of Wavelet's Coefficients and Support Vector Machine. *Journal of Mechanics in Medicine and Biology.* <https://doi.org/10.1142/S0219519420500360>.

[18] Taifi K, et al. Mammogram Classification Using Nonsampled Contourlet Transform and Gray-Level Co-Occurrence Matrix. *Crit Approaches to Inf Retr Res Glob.* 2020:239–55.

[19] Khan S, Hussain M, Aboalsamh H, Mathkour H, Bebis G, Zakariah M. Optimized Gabor features for mass classification in mammography. *Appl Soft Comput.* 2016; 44:267–280.

[20] Mughal B, Sharif M, Muhammad N, Saba T. A novel classification scheme to decline the mortality rate among women due to breast tumor. *Microsc Res Tech.* 2018. <https://doi.org/10.1002/jemt.22961>.

[21] Al-masni MA, et al. Simultaneous detection and classification of breast masses in digital mammograms via a deep learning YOLO-based CAD system. *Comput Methods Programs Biomed.* 2018; 157:85–94

[22] Benzebouchi NE, Azizi N, Ayadi K A. computer-aided diagnosis system for breast cancer using deep convolutional neural networks. In: *Computational intelligence in data mining* Springer, Singapore. *Advances in intelligent systems and computing.* 2019; 711.

[23] Agnes, S. Akila, J. Anitha, S. Immanuel Alex Pandian, and JDP. Classification of Mammogram Images Using Multiscale all Convolutional Neural Network (MA-CNN). *J Med Syst.* 2020; 44:30.

[24] Dabbaghchian S, Ghaemmaghami MP, Aghagolzadeh A. Feature extraction using discrete cosine transform and discrimination power analysis with a face recognition technology. *Pattern Recognition.* 2010; 43(4):1431–1440.

[25] Suckling J, Parker J, Dance D, et al. Mammographic Image Analysis Society (MIAS) database v1.21; 2015.

[26] Kshema J, George M, Dhas DAS. Preprocessing filters for mammogram images: a review. *IEEE Conference on Emerging Devices and Smart Systems;* Mar 3–4, 2017; Tamilnadu, India; 2017: 3–4.

[27] Sapate S, Talbar S. An overview of pectoral muscle extraction algorithms applied to digital mammograms. In: Dey N, Bhateja V, Hassanien A, eds. *Medical Imaging in Clinical Applications.* Cham: Springer. 2016:19–54.

[28] Adams R, Bischof L. Seeded region growing. *IEEE Trans Pattern Anal Mach Intell.* 1994;16(6):641–647.

[29] Cooley, J. W., & Tukey, J. W. (1965). An algorithm for the machine calculation of complex Fourier series. *Mathematics of computation,* 19(90), 297–301.

[30] Lu, Y., Schlosser, S., & Janeczko, M. (1993). Fourier descriptors and handwritten digit recognition. *Machine Vision and Applications,* 6(1), 25–34.

[31] Hamd, M. H., & Ahmed, S. K. (2017). Fourier descriptors for iris recognition. *International Journal of Computing and Digital Systems,* 6(05), 285–291.

[32] Wang C, Mai X, Lin G, Tan Kuo C. Classification for breast MRI using support vector machine. *International Conferences on Computer and Information Technology Workshops;* 8–



11 July 2008; Sydney, Australia: IEEE;  
2008: p. 362–367

[33] Vapnik V. *Statistical Learning Theory*. New York: Wiley; 1998.

[34] Singh S, Gupta PR. Breast cancer detection and classification using neural network. *Int J Adv Eng Sci Technol*. 2011; 6:4–9.

[35] Tang B, Kay S, He H, Toward. optimal feature selection in naive Bayes for text categorization. *IEEE Trans Knowl Data Eng*. 2016; 28:2508–2521.

[36] Altman, Naomi S. An introduction to kernel and nearest-neighbour non parametric regression. *The American Statistician*.1992;46(3):175–185. doi: 10.1080/00031305.1992.10475879.

[37] Singh VP, Srivastava S, Srivastava R. Effective mammogram classification based on center symmetric-LBP features in wavelet domain using random forest classifier. *Technol Health Care*. 2017; 1: 1–19.

[38] Elmoufidi A, et al. Automatic Detection of Suspicious Lesions in Digital X-ray Mammograms. In : El-Azouzi R, Menasche D, Sabir E, De Pellegrini F, Benjillali M, eds. *Advances in Ubiquitous Networking 2*. UNet 2016. *Lecture Notes in Electrical Engineering*, Singapore: Springer. 2017; 397.

[39] N. El-Sokary, et al. Computer-Aided Detection System for Breast Cancer Based on GMM and SVM. *Arab Journal of Nuclear Sciences and Applications*. 2019; 52(2):142–150.

[40] Luqman Ahmed et AL, Images data practices for Semantic Segmentation of Breast Cancer using Deep Neural Network. *Journal of Ambient Intelligence and Humanized Computing*. 2020. <https://doi.org/10.1007/s12652-020-01680-1>.